Tailoring Čerenkov second-harmonic generation in bulk nonlinear photonic crystal

Yan Sheng,[1,*] Vito Roppo,[2] Qian Kong,[1,3] Ksawery Kalinowski,[1] Qi Wang,[3] Crina Cojocaru,[2] Jose Trull,[2] and Wieslaw Krolikowski[1]

[1]*Laser Physics Center, Research School of Physics and Engineering, Australian National University, Canberra ACT 0200, Australia*

[2]*Departament de Fisica i Enginyeria Nuclear, Universitat Politecnica de Catalunya, Rambla Sant Nebridi, 08222 Terrassa, Barcelona, Spain*

[3]*Department of Physics, Shanghai University, Shanghai 200444, China*

**Corresponding author: ysh111@physics.anu.edu.au*

Received April 22, 2011; revised June 6, 2011; accepted June 8, 2011; posted June 9, 2011 (Doc. ID 146367); published July 1, 2011

We investigate theoretically the Čerenkov-type second-harmonic generation in two-dimensional *bulk* nonlinear photonic crystal with longitudinal modulation of the $\chi^{(2)}$ nonlinearity. We show that in this scheme the Čerenkov radiation can be achieved simultaneously at multiple directions with comparable intensities. The angles of emission are controllable by the spatial modulation of the nonlinearity. We propose a design of the periodically poled domain pattern, which maximizes the efficiency of the second-harmonic emission. © 2011 Optical Society of America

OCIS codes: 190.2620, 190.4410, 220.4000, 050.1940.

The second-harmonic generation (SHG), i.e., the conversion of two photons of the fundamental wave into a single photon at the doubled frequency, is widely used to create coherent light sources at new wavelength regions. The SHG occurs most efficiently when the phase matching (PM) condition is fully satisfied. This can be achieved in nonlinear photonic crystals (NPCs) [1,2]formed by ferroelectric domain reversal and using the quasi-PM technique [3–5]. The resulting one-dimensional (1D) or two-dimensional (2D) modulation to the sign of the second-order nonlinearity $\chi^{(2)}$ enables efficient SHG complying with the vectorial quasi-PM $2\mathbf{k}_1 + \mathbf{G} = \mathbf{k}_2$, where $\mathbf{G}$ is the reciprocal lattice vector and $\mathbf{k}_1$, $\mathbf{k}_2$ are the wave vectors of the fundamental and second harmonic (SH) waves, respectively [6,7]. Moreover, efficient SHG can also occur via Čerenkov-type interaction that involves only fulfilment of the longitudinal PM condition, i.e., $|\mathbf{k}_2|\cos\theta = 2|\mathbf{k}_1|$ with θ being the Čerenkov angle [8,9]. The generation of such a Čerenkov SHG is accessible in waveguide schemes utilizing the automatically achieved PM between the guided fundamental and radiated SH waves [10,11]. It is also possible to produce Čerenkov SHG in bulk NPC [12,13], for which the presence of $\chi^{(2)}$ modulation plays a key role as it enhances the intensity of the emission greatly [8,14,15].

So far the Čerenkov-type interaction in bulk NPC has led to the SHG only at fixed directions. With the propagation direction of the fundamental wave coinciding with ferroelectric domain walls (the boundaries between the $\chi^{(2)}$ and $-\chi^{(2)}$) [see Figs. 1(a) and 1(b)], the Čerenkov angle is determined by the scalar condition $\cos\theta = 2k_1/k_2 = n_1/n_2$, with n_1, n_2 being the refractive indices of the fundamental and SH waves. This is a consequence of the fact that $\chi^{(2)}$ is only modulated in the direction perpendicular to the beam propagation. Therefore, in order to be able to vary the Čerenkov emission angle, one has to modify the longitudinal PM condition by introducing the $\chi^{(2)}$ modulation along the propagation direction of the fundamental beam. In principle, this could be realized by employing a three-dimensional (3D) NPC [16], but the practical significance of this system is limited due to the technical difficulties in fabricating such 3D domain-inverted structures.

In this Letter, we propose an alternative way to employ a 2D NPC with the fundamental beam propagating in the plane of $\chi^{(2)}$ modulation [see Fig. 1(c)]. We show that in this geometry of interaction, the emission angles of the Čerenkov SH are associated with the period of $\chi^{(2)}$ modulation. We also consider the effect of different shapes of reversed domains on the conversion efficiency of the Čerenkov SHG. We show in this regard the performance of a chessboard-like structure is superior to that of the traditional 2D structures consisting of reversed domains of circular or square shapes.

We analyze the spatial evolution of the amplitude of the SH field, $A_2(x,y)$, considering the fundamental Gaussian beam propagating along the x axis, as schematically shown in Fig. 1(c). With assumptions of nondepletion of the fundamental wave (weak conversion efficiency) and slowly varying envelope of the SH wave, the $A_2(x,y)$ is governed by the equation:

$$\left(\frac{\partial}{\partial x} + \frac{i}{2k_2}\nabla_\perp^2\right)A_2(x,y) = -ig(x,y)\beta_2 A_1^2(y)e^{i\Delta kx}, \quad (1)$$

where $\Delta k = k_2 - 2k_1$; $A_1(y)$ is the amplitude of the fundamental field and for a Gaussian beam it reads $A_1(y) = A_0 e^{-y^2/w^2}$ with A_0 being the maximum pump amplitude at the center of the beam and w being the beam width; $\beta_2 = k_2\chi^{(2)}/(2n_2^2)$ is the nonlinear coupling coefficient;

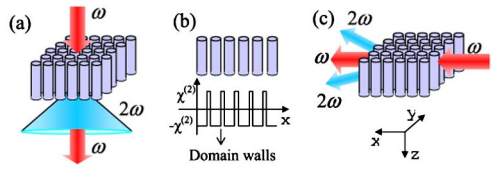

Fig. 1. (Color online) (a) Čerenkov SHG with fundamental beam propagating along domain walls. (b) Definition of domain walls. (c) Čerenkov SHG with fundamental beam propagating in the plane of $\chi^{(2)}$ modulation.

and $g(x,y)$ is the function characterizing the distribution of $\chi^{(2)}$.

To solve Eq. (1) we represent the amplitude $A_2(x,y)$ through its Fourier spectrum and express the function of $g(x,y)$ as a Fourier series. Then for the spectral density $S_2(x,\kappa_y) = |A_2(x,\kappa_y)|^2$ of the SH field, we have the following expression:

$$S_2(x,\kappa_y) = \pi w^2 x^2 \Gamma^2/2\left(\sum_{m,n=\pm1,\pm2,\ldots} g_{mn}\mathrm{sinc}[x(\Delta k + mG_x - \kappa_y^2/2k_2)/2] \times e^{-w^2(nG_y+\kappa_y)^2/8}\right)^2, \quad (2)$$

where $\Gamma = -i\beta_2 A_0^2$, $\mathrm{sinc}(y) = \sin(y)/y$, G_x, G_y are the primary reciprocal lattice vectors of the 2D periodic structure, and g_{mn} is the Fourier coefficient. From Eq. (2) one finds that when

$$\Delta k + mG_x - \kappa_y^2/2k_2 = 0, \quad (3)$$

the intensity of the SH grows quadratically with the propagation distance (x). For $\kappa_y^2/2k_2 \ll 1$ we obtain $k_2\cos\theta = 2k_1 + mG_x$. This relation represents the PM condition for Čerenkov SHG. We recover the standard case when either $m = 0$ or there is no longitudinal modulation of $\chi^{(2)}$ ($G_x = 0$). In Fig. 2(a) we plot the corresponding PM diagrams when $m = 0, \pm1$. It is seen that for a given wavelength, the emission of the Čerenkov SH can be observed at multiple directions that can be controlled by varying the period of $\chi^{(2)}$ modulation.

According to Eq. (2) the intensity of the Čerenkov SH is proportional to the strength of the relevant Fourier coefficient of the $\chi^{(2)}$ modulation. For 2D periodic NPC, this Fourier coefficient can be expressed as $g_{mn} = \frac{1}{C}\mathcal{F}(mG_x/2\pi, nG_y/2\pi)$, where C is the area of the unit cell and $\mathcal{F}$ denotes the Fourier transform of the motif function which defines the shape of the individual reversed domains [5]. Thus, to obtain the highest possible conversion efficiency for a given Čerenkov SHG, one should design the reversed domain shape such that it maximizes the relevant Fourier coefficients g_{mn}.

To illustrate this idea we concentrate below on three types of NPCs. The first two are the widely used structures consisting of a set of reversed domains in circular and rectangular shapes, as schematically shown in Fig. 2(b). The radius and the side length of the reversed domains are denoted as r and l, respectively. In addition, we also consider a chessboard-like structure [see the bottom of Fig. 2(b)]. The fundamental difference between the chessboard and the other two patterns is that the domain walls, whose presence enhances the Čerenkov SH emission, are densely distributed in the former case and only sparsely in the latter.

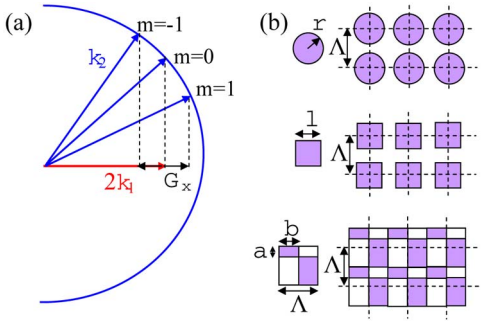

Fig. 2. (Color online) (a) Čerenkov SHG with $m = 0, \pm1$. (b) Different shapes of the reversed domains: circular, square, and chessboard-like structures.

In the left column of Fig. 3 we show the far-field SH angular distribution calculated for the NPC with different shapes of the reversed domains, i.e., the circular, the square, and the chessboard-like structures. In the calculations we assume the reversed domains are formed in stoichiometric lithium tantalate crystals and arranged into a square lattice of period $\Lambda = 7.5\,\mu$m. We use a fundamental beam of wavelength $\lambda_1 = 1.48\,\mu$m and beam width $w = 15\,\mu$m. In order to fairly compare the performances of these three structures, we chose for each of them the duty cycle such that it maximizes the Čerenkov SHG for the zero order ($m = 0$) emission. Hence, $r/\Lambda = 0.469$ for the circular, $l/\Lambda = 0.391$ for the square, and $a/\Lambda = 0.05$, $b/\Lambda = 0.125$ for the chessboard patterns [see the right column of Fig. 3(b)]. Actually the condition $a/\Lambda = 0.05$ is not optimal for the chessboard structure, as it allows around 82% of the maximum efficiency. The optimum occurs when $a/\Lambda = 0.0$ (or 1.0), as shown in Fig. 3(f), which means the rectangles along the x direction merge into a continuous line, i.e., the 2D structure becomes, in fact, a 1D structure. Here we sacrifice some efficiency for the sake of additional degree of freedom to produce multiple Čerenkov SH due to the longitudinal modulation of $\chi^{(2)}$. It is seen from the left column of Fig. 3 the SH is emitted symmetrically with respect to the direction of the fundamental beam. Its maximum at $\kappa_y = \pm3.48\,\mu\mathrm{m}^{-1}$ corresponds to the angles of $\pm10.96°$. These values are in excellent agreement with the Čerenkov angles (10.92°) predicted by Eq. (3) when $m = 0$ and using the refractive indices reported in [17]. These results

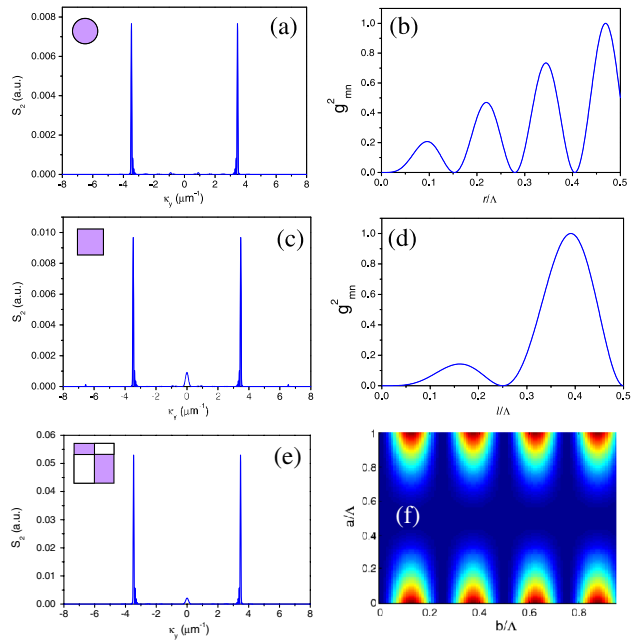

Fig. 3. (Color online) Left column: Čerenkov SHG in 2D NPC formed by circular, square, and chessboard-like reversed domains. Right column: the effect of duty cycle.

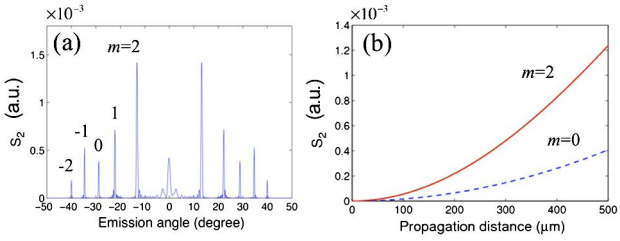

Fig. 4. (Color online) (a) Čerenkov SHG at multiple directions. (b) The generated SH signal as a function of propagation distance.

also indicate that the Čerenkov SH generated in the chessboard-like structure is the most efficient, while that produced by the circular reversed domains is the weakest. Our calculation shows that for a 10 mm long chessboard sample, a 2.8% efficiency of the Čerenkov SHG could be achieved with pump intensity of $500\,\mathrm{MW/cm^2}$.

The physical origin of such different responses to the Čerenkov SHG can be attributed to the different distributions of domain walls in these three structures. We have previously verified that the Čerenkov SHG occurs efficiently only on the domain wall regions [14]. Moreover, only the domain walls that are parallel to the propagation direction of the fundamental wave contribute to the Čerenkov SHG. Therefore, for the circular shape of reversed domains, only a very small part of domain walls participates in the Čerenkov emission. On the other hand, in the chessboard structure, the domain walls are continuously redistributed across the whole sample and along the fundamental wave and hence they all contribute to the Čerenkov SHG.

Finally, we design the chessboard-like structure, which leads to simultaneous generation of Čerenkov SHG at multiple directions with comparable intensities, as determined by the PM relation Eq. (3). The period of the chessboard structure is $\Lambda = 29\,\mu$m and the duty cycle is $a/\Lambda = b/\Lambda = 0.666$. The SHG output calculated using Eq. (2) after a $500\,\mu$m propagation distance is shown in Fig. 4(a), with fundamental wavelength $\lambda_1 = 1.2\,\mu$m. The emission angles of these SH waves agree with those defined by Eq. (3), with $m = 0, \pm 1, \pm 2$, respectively. In Fig. 4(b) we show the dependence of the output of two Čerenkov SH ($m = 0$, and $m = 2$) on the length of the NPC. It is clear that the Čerenkov SH radiation, which is defined by the longitudinal PM condition only, is coherently growing through the sample like a fully phase matched process.

In conclusion, we have studied the Čerenkov SHG in 2D NPC with fundamental beam propagating in the plane of $\chi^{(2)}$ modulation. We show that in this case the emission angles of the Čerenkov SH is controllable by the period of the nonlinearity modulation. We also proposed a chessboard structure, which leads to much higher efficiency of the Čerenkov SHG than the commonly used 2D structures with circular or square shapes of reversed domains.

The authors acknowledge the Australian Research Council for financial support. V. Roppo thanks Army Research Office (W911NF-10-2-0105) for the partial financial support.

References

1. V. Berger, Phys. Rev. Lett. **81**, 4136 (1998).
2. N. G. R. Broderick, G. W. Ross, H. L. Offerhaus, D. J. Richardson, and D. C. Hanna, Phys. Rev. Lett. **84**, 4345 (2000).
3. J. A. Amstrong, N. Bloembergen, J. Ducuing, and P. S. Pershan, Phys. Rev. **127**, 1918 (1962).
4. S. Zhu, Y. Zhu, and N. Ming, Science **278**, 843 (1997).
5. A. Arie, N. Habshoosh, and A. Bahabad, Opt. Quantum Electron. **39**, 361 (2007).
6. Y. Sheng, J. Dou, B. Ma, B. Cheng, and D. Zhang, Appl. Phys. Lett. **91**, 011101 (2007).
7. A. Arie and N. Voloch, Laser Photon. Rev. **4**, 355 (2010).
8. A. Fragemann, V. Pasiskevicus, and F. Laurell, Appl. Phys. Lett. **85**, 375 (2004).
9. S. M. Saltiel, Y. Sheng, N. Bloch, D. N. Neshev, W. Krolikowski, A. Arie, K. Koynov, and Y. S. Kivshar, IEEE J. Quantum Electron. **45**, 1465 (2009).
10. P. K. Tien, R. Ulrich, and R. J. Martin, Appl. Phys. Lett. **17**, 447 (1970).
11. Y. Zhang, Z. D. Gao, Z. Qi, S. N. Zhu, and N. B. Ming, Phys. Rev. Lett. **100**, 163904 (2008).
12. Y. Sheng, S. M. Saltiel, W. Krolikowski, A. Arie, K. Koynov, and Y. S. Kivshar, Opt. Lett. **35,**1317 (2010).
13. W. Wang, Y. Sheng, Y. Kong, A. Arie, and W. Krolikowski, Opt. Lett. **35**, 3790 (2010).
14. Y. Sheng, A. Best, H. Butt, W. Krolikowski, A. Arie, and K. Koynov, Opt. Express **18**, 16539 (2010).
15. J. Chen and X. Chen, Opt. Express **18**, 15597 (2010).
16. J. Chen and X. Chen, J. Opt. Soc. Am. B **28**, 241 (2011).
17. I. Dolev, A. Ganany-Padowicz, O. Gayer, A. Arie, J. Mangin, and G. Gadret, Appl. Phys. B **96**, 423 (2009).